https://adv-j-sci-eng.com

Electronic Structure Study of Sn-Substituted InP Semiconductor

Osman Murat Ozkendir[1],✉

Adv-J-Sci-Eng

ABSTRACT. Indium phosphide (InP) semiconductor is a well-known binary semiconductor. The electronic properties have helped this material gain high popularity due to its desired semiconductor properties. In this study, the InP semiconductor was processed with Sn substitution in the indium coordination to probe the influence of electronic interplays on the electronic properties of semiconductor materials. The study is carried by the x-ray absorption fine structure (XAFS) spectroscopy calculations. Tin is one of the most popular metal used in recent technology due to its potential to emerge desired electronic properties. The calculations were performed by the commercial code FEFF 8.2 for a 10 Å thick cluster. The results showed a possible application of Sn substitution can yield better semiconductor properties in an electronic device application.

Keywords: Crystal structure; Electronic structure; Semiconductor; Absorption spectroscopy.

INTRODUCTION

Semiconductors are the main materials of the electronic devices that are a major part of our daily life and work. Several attempts have been dedicated to find electronic and structural properties of combination of atoms of group III of periodic table with phosphorus atom to form III-P hetero nanostructures.[1-7] Moreover, impurities have been also considered as a driving factor to modify the properties of III-P structures for specific purposes.[8-12] Indium phosphide (InP) materials with properties such as low dielectric, low densities, extremely high thermal conductivities, and wide band-gap have placed InP semiconductors in an important place among other conductors.[13] In this way, it has made it possible to use electronic devices with the required

features in environments where they are needed. InP crystallizes in cubic (zinc blende) structure and owns a space group of "*Fm3m*".[14] The lattice parameters are reported by Iandelli in 1940 as; a: 5.861 Å. The sketched crystal structure of the InP semiconductor is given in Fig. 1 (a) and (b).[15] Indium phosphide has vast area of use like, high frequency field effect transistors, nanowire solutions for solar cells and tunneling diodes.[13] In this study, XAFS calculations were performed to investigate the electronic structure properties of the InP semiconductor material and also the influence of Sn substitution on the electronic interplay that takes place in the molecular bonding. The technique XAFS is an expanded version of x-ray absorption spectroscopy (XAS) which is a popular method for determining the local geometric and/or electronic structure of materials. Thus, for an XAFS study, the data should be analyzed in two main sections; XANES (X-ray Absorption Near Edge Structure) and EXAFS (Extended-XAFS). The XANES part yield data for the chemical bonding, local geometry, electronic structure properties, while EXAFS data yields information about the atomic coordination and bond distances between the atoms.

MATERIALS AND METHODS

The calculations were performed to probe the electronic interplays between indium valence electrons and its neighboring atoms (In and P). For this purpose, In K-edge x-ray absorption fine structure (XAFS) calculations of the zinc blende InP clusters were performed by using FEFF 8.2 code, which is based on real space multiple scattering approach.[16] The

✉ Corresponding author.
  E-mail address: ozkendir@gmail.com (O.M. Ozkendir)

[1] School of Graduate Programs, Tarsus University, Tarsus, Turkey

[2] Department of Natural and Mathematical Sciences, Faculty of Engineering, Tarsus University, Tarsus, Turkey

calculations need an input file, where electronic energy details, computational cards, and crystal data are presented. Thus, an input file was created by using the ATOMS package, which is a part of the IFEFFIT Shell.[17-19] The calculations were done for 10 angstroms thick zinc blende InP cluster that is containing 159 atoms (In and P). For the Sn substituted material, 10 angstroms thick zinc blende $In_{0.80}Sn_{0.20}P$ clusters were created with 159 atoms (In, Sn and P). The tin atoms were localized in indium coordination in a ratio of In:

Sn as 4:1, respectively. Besides, a metal indium cluster (10 angstroms containing 161 atoms) were created as a reference for the calculation. The crystal data for the created indium metal was in tetragonal with a space group of "*i4/mmm*" and the lattice parameters were; a = 3.2446 Å, b = 3.2446 Å, c = 4.9367 Å. During the calculations, backscattering and phase shifts with single and multiple scattering paths have been calculated to obtain the EXAFS spectra for the room temperature condition.
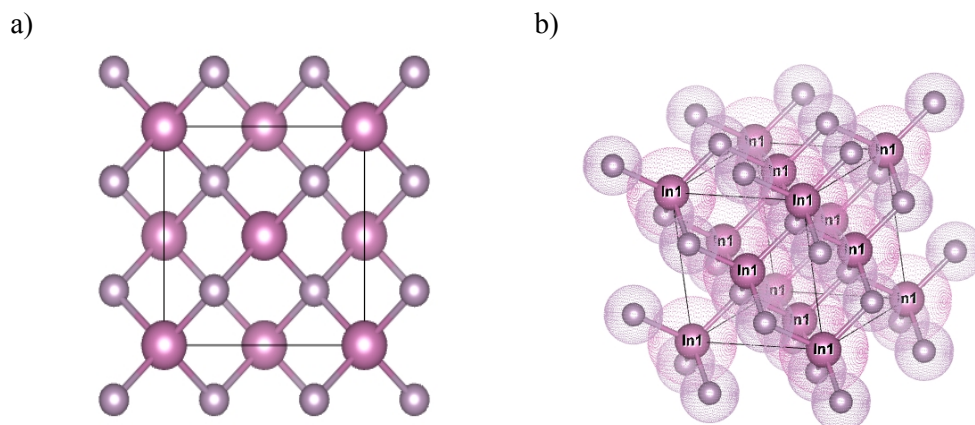
a)
b)

Fig. 1: Crystal structure of InP from; a) z-axis b) general view.
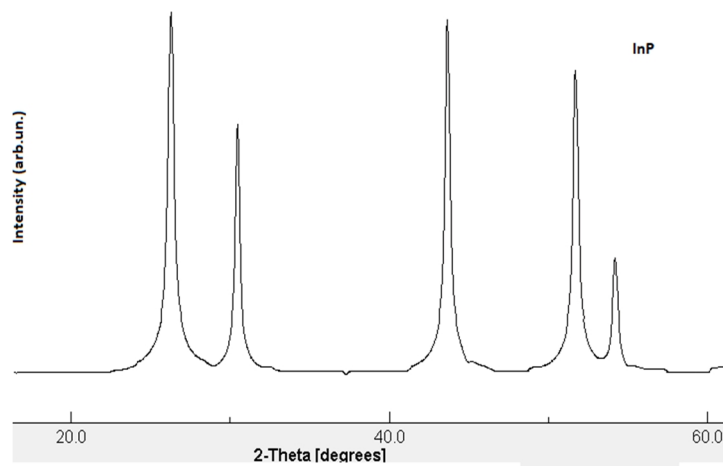

Fig. 2: X-ray diffraction pattern (XRD) created by the crystal card from Iandelli.[14]

RESULTS AND DISCUSSION

In the InP nanostructures, indium atoms possess In^{3+} ionic state, while phosphide atoms possess P^{3-} ionic state. The powder diffraction pattern for the InP semiconductor was created by using the crystal data card of Iandelli[14] and sketched as given in Fig. 2 (taken by the MAUD program).[20]

The created XRD pattern is a reference card for the zinc blende InP semiconductor material. The peak features and sharp intensities address the cubic geometry formed

by the In-P atoms. The mechanisms played by the valence electrons between two neighbor atoms can be best probed by the electronic structure study by the XAFS technique. The electronic ground state of the indium atom is "*[Kr] 4d^{10} 5s^2 5p^1*" and when it is ionized to In^{3+} its electronic configuration becomes "*[Kr] 4d^{10}*". So, indium could be ionized up to In^{3+} and above this ionization behaves like a noble gas order. Based on the electron configuration, the ground electronic state for phosphorus is "*[Ne] 3s^2 3p^3*" and

during ionized state it gains electrons from indium and filled up the *3p* state.

The influence of tin metal on the electronic and crystal properties of the InP semiconductor material can be best studied by the XAFS (XANES and EXAFS) technique. In K-edge absorption spectra is given in Fig. 3. K-edge of an atom corresponds to the Shell of the 1s electrons and K-edge absorption spectra is a result of excited *1s* electrons transition to the unoccupied valence "*5p*" levels. For In^{3+} ions, *5s* level is located below the *5p* levels with a lower energy and it is unoccupied. However, quantum selection rules forbid the transition of electrons' that have the same angular momentum and are the same, i.e., *Δl = ±1*. Thus the main route for the excited 1s electrons should be the unoccupied *5p* levels above the valence level. In K-edge absorption spectra of the zinc blende InP begin to rise at 27.91 keV and the main edge gives a maximum at 27.94 keV and this peak is a result of *1s—›5p* transition. The spectra welcome us with a tiny pre-edge structure that is familiar for indium spectra. However, below the main edge, a sharp-peaked weak edge structure is observed at 27.924 keV as a pre-edge. The pre-edge structure indicates the occurrence of a forbidden transition which points out the mechanism happened out of quantum selection rules. This can be due to the hybridization of (In) *5s-3p* (P) neighboring levels and lowering the built molecular band.
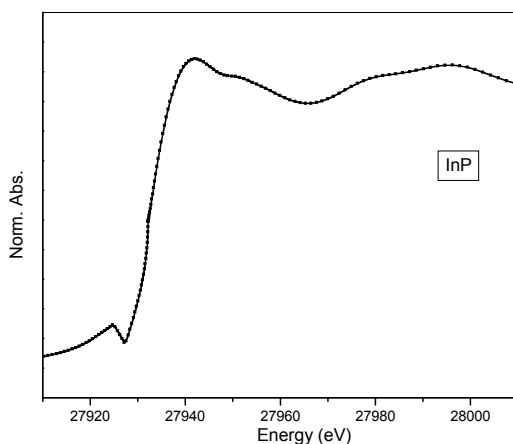
Fig. 3: In K-edge X-ray absorption spectra (XAS) of the InP semiconductor material.

To reveal the molecular interactions in the InP and $In_{0.80}Sn_{0.20}P$ semiconductors, In K-edge XAS spectra are given in Fig. 4 with In K-edge spectra of the In metal as a reference. In Fig. 4, the pre-edge part of the spectra clearly shows the influence of the *p*-levels on the unoccupied s and p-levels of indium. In metal has only one type of atom in its neighborhood (In) and that

avoids indium outer shell electrons to couple strongly to build up hybridized molecular bands. So, In K-edge spectra of the In metal has a smooth rise to the main edge without any pre-edge structure. The main edge peak of the metal indium has a maximum at 27.937 keV, which is 3 eV lower than InP. The inset in Fig. 4 clearly shows the shift in the energy decrease. The pre-edge feature in the Sn substituted material is stronger than the pure InP material. Electronic configuration of the Sn^{3+} ions is "*[Kr] $4d^{10}$ $5s^1$ $5p^0$*" and the one electron makes the tin atoms unstable. Thus, to become more stable, Sn^{3+} atoms have coupled more strongly to build up a hybridized level. The rest part of the Sn substituted InP has a high agreement with the parent InP, which points out the adaptation of the tin atoms in the crystal structure and supporting the electronic behaviors of the InP semiconductor materials. The behavior of the Sn atoms substituted in the In coordination can be traceable by analyzing the extended part of the XAFS spectra, i.e., EXAFS.
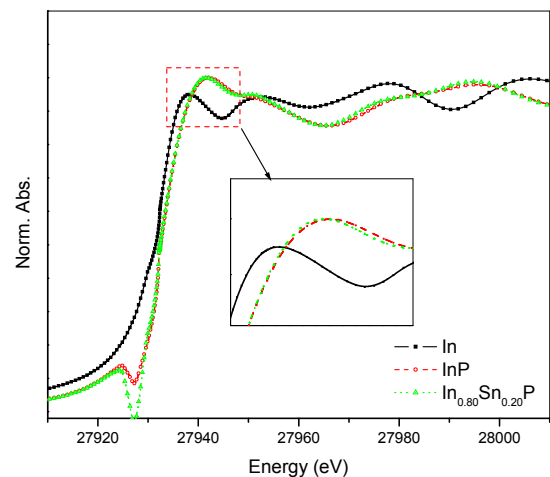
Fig. 4: Compared XAS spectra of the In K-edge of the In metal, InP and $In_{0.80}Sn_{0.20}P$ material.

EXAFS is a powerful tool to study the atomic localization and its data lays above 40-70 eV of the main absorption edge in the XAFS spectra. The mechanism of the fluctuations in the EXAFS part of the XAFS spectra is a result of the emitted core electron when it is excited with a photon that has an energy higher than the binding energy. The excess energy is used as the kinetic energy that allows it to travel among its nearest neighbors and create signals from the "scattering interaction". During the scattering, the wave-functions of the incoming and outgoing photoelectrons interfere and cause fluctuations. The fluctuations carry information about the atomic types and bonding

distances of the scattered electrons (photoelectron). For the EXAFS study, the fluctuating part of the spectra should be extracted and analyzed. The EXAFS scattering data of the In metal, InP and $In_{0.80}Sn_{0.20}P$ material are given in Fig. 5 in comparison.
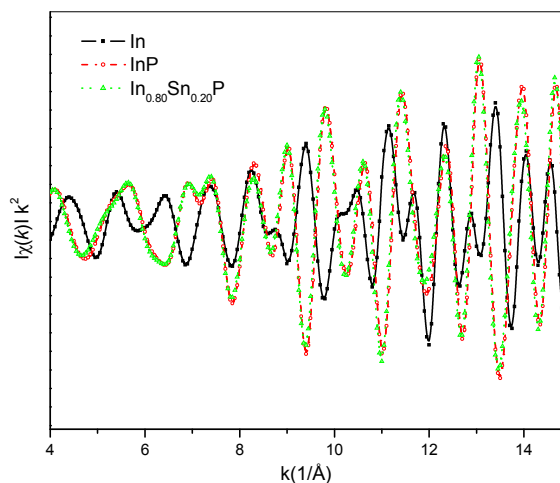

Fig. 5: Compared EXAFS spectra of the In metal, InP and $In_{0.80}Sn_{0.20}P$ material.

In Fig. 5, the scattering intensity of the metal In atoms has an agreement in the shape of the signal envelope and similar peak features. Also, a very high agreement between InP and $In_{0.80}Sn_{0.20}P$ materials' scattering intensities emphasizes the similar crystal structure properties between two crystals, even one containing a different atom type, Sn. As wave number k and the wavelength λ according to the ratio of "$k=1/\lambda$", the powerful scattering intensities mean strong scattering interactions in the vicinity of the source In atom of the photoelectrons. The Fourier transform (FT) of the scattering intensity data which was extracted from the XAFS tail spectra yields the real space atomic distances from the source atom (In). The FT of the spectra is called as the radial distribution function (RDF) which is related to the atomic distances of the neighboring atoms from the source atom on a one dimensional axis. Here, atoms may have the same distance but located with different angles in three dimensional real space cause displacements on the 1D axis and cause broadening on the peak structures. The compared RDF of the In metal, InP and $In_{0.80}Sn_{0.20}P$ material are given in Fig. 6.

To identify the exact atomic distances (bond lengths) fits should be performed which are generated during the EXAFS calculations. According to the fit results, the nearest neighbor of the In atoms in the In metal was determined at 3.24 Å. The weak peak features are generated from the multiple scattering processes. The nearest neighbors of the In metal, which is the source atom in the process were determined as; four P atoms at a distance of 2.54 Å and 12 In atoms at distance 4.15 Å.
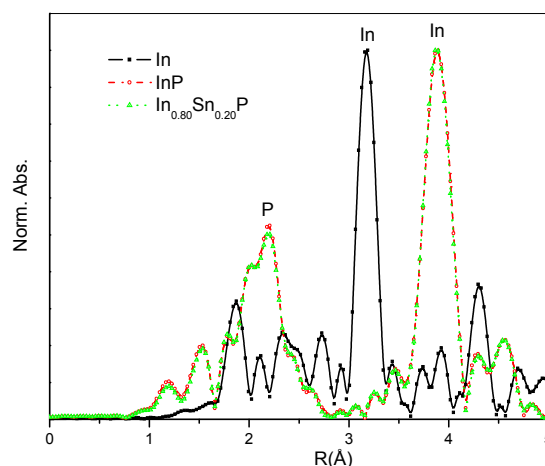
Fig. 6: Compared RDF of the In metal, InP and $In_{0.80}Sn_{0.20}P$ material.

Sn atoms seem to sit in the In coordination in the $In_{0.80}Sn_{0.20}P$ material and the high agreement and symmetry in peak structures confirm this phenomenon. So, Sn atoms can be said to sit at a distance of 4.15 Å among other In atoms.

CONCLUSION

In this study, Sn substituted InP semiconductor material was studied to probe the influence of Sn substitution on the electronic properties of the In atoms. Due to similar ionic properties of tin and indium ions, similar spectral features were observed. Sn is the neighbor of the indium atoms in the periodic table and shows similar characteristics. Thus, a stronger pre-edge feature was observed on the XAS spectra of the In K-edge in $In_{0.80}Sn_{0.20}P$ material due to the supporting behavior of the tin atoms in building up a hybridized molecular band with a lower energy level.

REFERENCES

1. Mirzaei M, Mirzaei M. A computational study of gallium phosphide nanotubes. Physica E 2011;43:1343-1345.
2. Mirzaei M, Mirzaei M. Aluminum phosphide nanotubes: Density functional calculations of aluminum-27 and phosphorus-31 chemical shielding parameters. J. Mol. Struct. THEOCHEM. 2010;951:69-71.
3. Mirzaei M. A computational NMR study of boron phosphide nanotubes. Z. Naturforsch. A 2010;65:844-848.

4. Mirzaei M, Mirzaei M. A computational study of aluminum phosphide. Int. J. Quant. Chem. 2011;111:3851-3855.

5. Mirzaei M, Yousefi M, Meskinfam M. Studying (n, 0) and (m, m) GaP nanotubes (n= 3–10 and m= 2–6) through DFT calculations of Ga-69 quadrupole coupling constants. Solid State Sci. 2012;14:801-804.

6. Mirzaei M, Mirzaei M. DFT calculations of NMR properties for GaP nanotubes. Monatsh. Chem. 2011;142:111-114.

7. Mirzaei M, Giahi M. Computational studies on boron nitride and boron phosphide nanotubes: density functional calculations of boron-11 electric field gradient tensors. Physica E 2010;42:1667-1669.

8. Mirzaei M. Carbon doped boron phosphide nanotubes: a computational study. J. Mol. Model. 2011;17:89-96.

9. Mirzaei M, Meskinfam M. Computational studies of effects of tubular lengths on the NMR properties of pristine and carbon decorated boron phosphide nanotubes. Solid State Sci. 2011;13:1926-1930.

10. Mirzaei M, Mirzaei M. A theoretical study of boron-doped aluminum phosphide nanotubes. Comput. Theor. Chem. 2011;963:294-297.

11. Mirzaei M, Aezami A, Mirzaei M. A computational study of silicon-doped aluminum phosphide nanotubes. Physica B 2011;406:84-87.

12. Mirzaei M, Mirzaei M. The C-doped AlP nanotubes: A computational study. Solid State Sci. 2011;13:244-250.

13. Okbi F, Lakel S, Benramache S, Almi K. First principles study on electronic structure and optical properties of ternary semiconductor $In_xAl_{1-x}P$ alloys. Semiconduct. 2020:54:58-66.

14. Iandelli A. Sulla struttura dei composti InP. Gazzet. Chim. Italian.1940;70:58-62.

15. Momma K, Izumi F. VESTA 3 for three-dimensional visualization of crystal, volumetric and morphology data, J. Appl. Crystallogr. 2011;44:1272-1276.

16. Ankudinov AL, Ravel B, Rehr JJ, Conradson SD. Relativistic calculations of spin-dependent x-ray-absorption spectra. Phys. Rev. B 1997;56:R1712.

17. Newville M. IFEFFIT: interactive XAFS analysis and FEFF fitting. J. Synch. Rad. 2001;8:322-324

18. Ozkendir OM, Gunaydin S, Mirzaei M. Electronic structure study of the $LiBC_3$ borocarbide graphene material. Adv. J. Chem. B 2019;1:37-41.

19. Ozkendir OM. Boron activity in metal containing materials. Adv. J. Chem. B 2020;2:48-54.

20. Lutterotti L, Bortolotti M. Object oriented programming and fast computation techniques in Maud, a program for powder diffraction analysis written in java. IUCr Compcomm. Newslett. 2003;1:43-50.

How to cite this article: Ozkendir OM. Electronic structure study of Sn-substituted InP semiconductor. Adv. J. Sci. Eng. 2020;1(1):7-11.